2002-04

Large-Scale Forcing of the Agulhas Variability: The Seasonal Cycle

Matano, R.P.

Large-Scale Forcing of the Agulhas Variability: The Seasonal Cycle

R. P. Matano, E. J. Beier, and P. T. Strub

College of Oceanic and Atmospheric Sciences, Oregon State University, Corvallis, Oregon

R. Tokmakian

Department of Oceanography, Naval Postgraduate School, Monterey, California

ABSTRACT

In this article the authors examine the kinematics and dynamics of the seasonal cycle in the western Indian Ocean in an eddy-permitting global simulation [Parallel Ocean Circulation Model, model run 4C (POCM-4C)]. Seasonal changes of the transport of the Agulhas Current are linked to the large-scale circulation in the tropical region. According to the model, the Agulhas Current transport has a seasonal variation with a maximum at the transition between the austral winter and the austral spring and a minimum between the austral summer and the austral autumn. Regional and basin-scale mass balances indicate that although the mean flow of the Agulhas Current has a substantial contribution from the Indonesian Throughflow, there appears to be no dynamical linkage between the seasonal oscillations of these two currents. Instead, evidence was found that the seasonal cycle of the western Indian Ocean is the result of the oscillation of barotropic modes forced directly by the wind.

1. Introduction

In a recent letter, Biastoch et al. (1999) noted the existence, in a large-scale simulation of the South Indian Ocean, of a seasonal oscillation of the Agulhas transport and suggested that it might be forced by variations of the wind-driven forcing. According to these results the Agulhas transport has a maximum at the transition between the austral winter and the austral spring and a minimum between the austral summer and the austral autumn. Although there is no evidence to prove the existence of such a cycle, Biastoch et al. (1999) noted that this might be due to the scant in situ observations existing in the region. As for the origins of the seasonal signal, Biastoch et al. (1999) speculated that it might be associated with meridional displacements of the South Indian anticyclone.

The results of Biastoch et al. (1999) suggest the possibility that the variabilities of the tropical and subtropical gyres may be linked at seasonal and interannual timescales. We will investigate these matters by analyzing the results of a different numerical experiment. Our objective is to elucidate the dynamical processes by which the large-scale circulation influences the variability of the Agulhas region. In the first part of this study we will analyze the kinematics and dynamics of

the annual cycle simulated in a global, eddy-permitting, numerical experiment, while in a forthcoming article we will compare the model results with altimeter data.

This article is organized as follows: In section 2, we briefly describe the characteristics of the numerical model to be analyzed. In section 3 we describe the model results starting with a characterization of the mean circulation and the seasonal cycle, followed by a discussion of the dynamical processes responsible for the observed adjustment. In section 4 we summarize our results and discuss their relevance to existing observations.

2. Model description

The numerical experiment to be discussed was performed by R. Tokmakian using the Parallel Ocean Circulation Model (POCM). The model equations were discretized to a Mercator grid with an average horizontal grid spacing of $\frac{1}{4}°$ and 20 vertical levels. The bottom topography of the model was derived from the $\frac{1}{12}°$ 5-min gridded Earth Topography dataset (ETOPO5). A detailed description of the model equations and numerical algorithms can be found in Stammer et al. (1996, and references therein. Our analysis will be focused on the experiment POCM-4C, which was run for a 19-yr period. From 1979 to 1994 the model was forced with atmospheric fluxes derived from the European Centre for Medium-Range Weather Forecasts (ECMWF) reanalysis; after that time period the forcing fluxes were replaced with operational ECMWF datasets. For the pur-

Corresponding author address: Dr. R. P. Matano, College of Oceanic and Atmospheric Sciences, Oregon State University, Corvallis, OR 97331-5503.
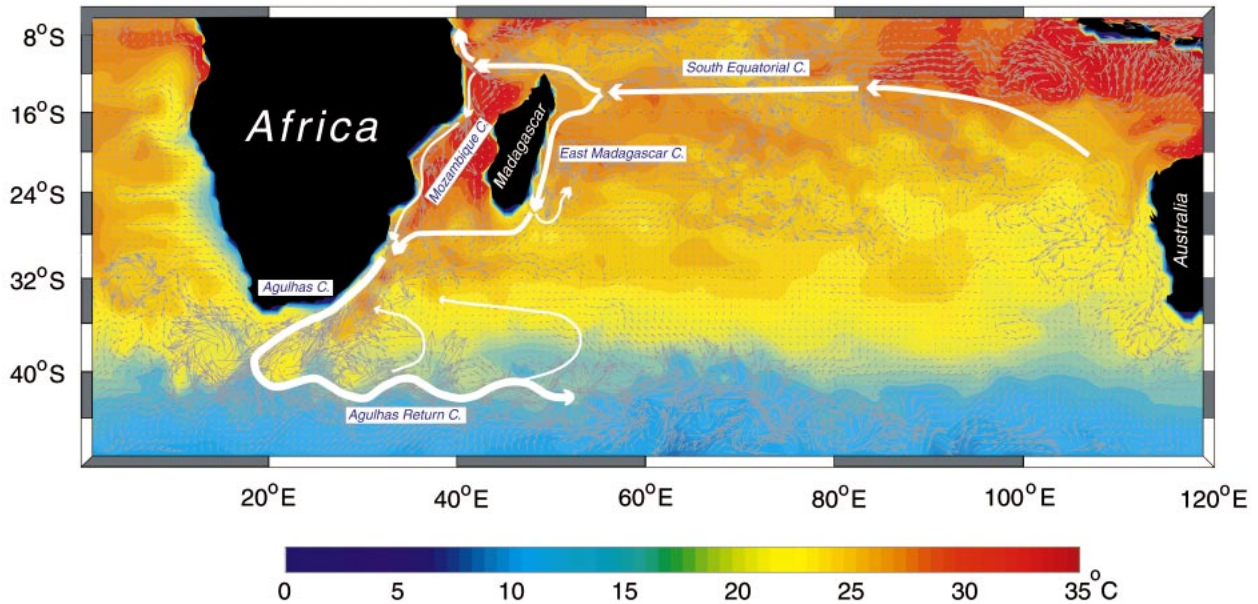E-mail: rmatano@oce.orst.edu

FIG. 1. Snapshot of the upper velocities and sea surface temperatures in the POCM underlying a schematic representation of the mean circulation.

poses of this article we use 3-day averages (separated by 9 days) of model outputs of temperature, salinity, velocity, and sea surface height (SSH) corresponding to the period 1986–98.

3. Kinematics

Figure 1 illustrates the general features of the South Indian Ocean circulation in a synoptic view of the POCM's upper velocities and sea surface temperatures (SSTs). Although the energy levels of the model's upper circulation are known to be lower than those observed from satellite altimetry, the POCM has been otherwise favorably compared with altimetric SSH observations (Stammer et al. 1996). The equatorial region of the south Indian Ocean is dominated by the broad, eastward flow of the South Equatorial Current, which extends from approximately 15° to 8°S. The South Equatorial Current is not a single, broad current, but rather several narrow jets that split and coalesce at locations marked by steep topographic formations. After impinging on the continental boundary, a portion of the South Equatorial Current diverts poleward to feed the Mozambique Current, which afterward merges with the East Madagascar Current along the coast of Africa to form the Agulhas Current. The confluence of the Mozambique Current and the East Madagascar Current generates the narrow, but well-defined, poleward flow of the Agulhas Current. After leaving the continental boundary, the Agulhas Current retroflects and returns to the Indian Ocean as a highly variable eastward-flowing jet, the Agulhas Return Current. At the western end of the Agulhas retroflection there is intermittent formation of eddies, most

of which are entrained into the subtropical gyre of the South Atlantic Ocean.

a. The mean circulation

As a general reference for our discussion, Fig. 2 shows the POCM's time- and depth-averaged velocities in the southwestern Indian sector. Superimposed on these mean velocities are the locations at which we calculate the volume transports of the main regional currents—namely, the North Madagascar, Mozambique, East Madagascar, and Agulhas Currents. Table 1 compares the volume transports shown in Fig. 2 with values estimated from in situ (current meters or LADCP) and satellite observations. The standard deviations included in Table 1 indicate that the transports derived from the POCM are statistically undistinguishable from the observed values. In this regard it should be noted that the comparison between model and observations is hampered by the fact that, while the observational values are based on relatively short records, the values calculated from the model represent climatological averages.

The transport of the Agulhas Current at 32°S is approximately 43 Sv (Sv $\equiv 10^6$ m^3 s^{-1}) It comprises 30 Sv drawn from the East Madagascar Current and 12 Sv from the Mozambique Current. The mean transport derived from the POCM is smaller than the 85 Sv estimated by Toole and Warren (1993) and the 78 Sv estimated by Beal and Bryden (1999). A portion of the discrepancy is attributed to differences in the sections where the Agulhas transport was calculated. In Fig. 2 we used a strictly zonal section that measures only the
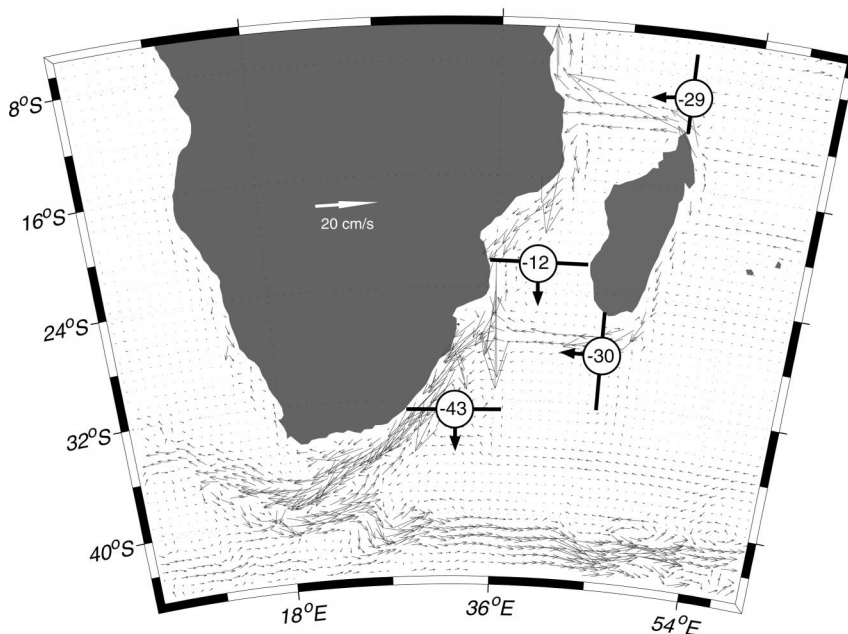
FIG. 2. Volume transports in the southwestern Indian Ocean superimposed on the climatological mean velocity vectors. The transports are quoted in Sverdrups.

contributions from the Mozambique Channel and the East Madagascar Current, while the slanted sections used by Toole and Warren (1993) and Beal and Bryden (1999) include contributions from the inertial recirculation cell. The volume transport estimated by the POCM using the same section as Beal and Bryden (1999) is 58 Sv ± 11 Sv.

To illustrate the general variability of the Agulhas transport Fig. 3 shows a time series calculated along the section used by Beal and Bryden (1993). Peaks of the transport of more than 90 Sv characterize the Agulhas variability. These peaks are generally associated with

the passage of eddies originating in the far field (Biastoch and Krauss 1999; Schouten et al. 2002); or with local instability phenomena (de Ruijter et al. 1999; van Leeuwen et al. 2000).

The transport of the Mozambique Current predicted by the POCM is approximately twice the value estimated by Stramma and Lutjeharms (1997), and Fu (1986). In absolute values however, the 7 Sv difference between model and observations is within the expected margin of error because of the high variability of the circulation within the Mozambique Channel (Lutjeharms et al. 2000; de Ruijter et al. 2002). Although the

TABLE 1. A comparison between the current transports simulated by the POCM and observations. The transports and standard deviations are given in Sverdrups.

| Current	Author	Transport	Reference level	POCM
North Madagascar	Swallow et al. (1988)	29	1100 m	29±11
	Schott et al. (1988)	27±9	Current meter	
Mozambique	Harris (1972)	10	~2500 m ($\sigma_t = 27.2$)	
	Stramma and Lutjeharms (1997)	5	1000 m	12±7
	Fu (1986)	6	Satellite	
	de Ruijter et al. (2002)	12	LADCP	
Agulhas	Gründlingh (1980)	20–40		
	Gordon et al. (1987)	49	1500 m	
	Stramma and Lutjeharms (1997)	45	1000 m	43±8
	Toole and Warren (1993)	85	2000 m	
	Beal and Bryden (1999)	78±3	Current meter	58±11
East Madagascar	Stramma and Lutjeharms (1997)	25	1000 m	
	Schott et al. (1988)	20±6	Current meter	
	Swallow et al. (1988)	20	1100 m	30±5
	Lutjeharms et al. (1981)	41	2000 m	
	Harris (1972)	35	~2500 m ($\sigma_t = 27.2$)	
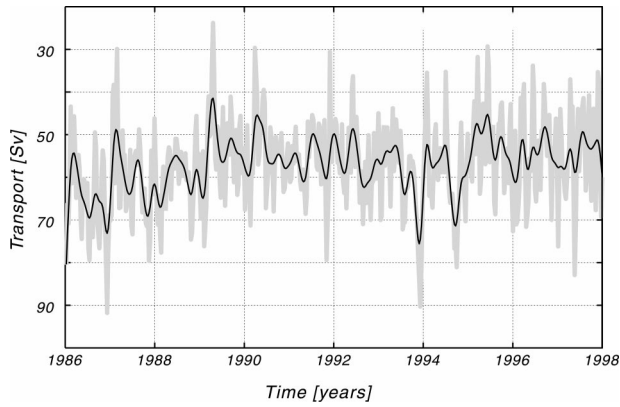
FIG. 3. Time series of the volume transport of the Agulhas Current in the section extending from 31°S, 30.2°E to 32.36°S, 32.2°E. The gray shading marks the time evolution of the instantaneous velocities while the thin black line is a running mean.

differences between model and in situ transport estimates may be relatively small, the 12 Sv of poleward transport through the Mozambique Channel predicted by the POCM is too high to be a purely wind-driven flow. In fact, a calculation using the "rule of the island" (Godfrey 1989) shows that only 2.2 Sv can be accounted for by the wind-driven circulation. The genesis of the additional 9.8 SV is suggested by a volume balance of the entire tropical region (Fig. 4), which indicates that the outflow of tropical waters through the Mozambique Channel is compensated by an inflow of Pacific waters through the Indonesian passages. The value of the Indonesian Throughflow estimated by the POCM is within the 5–15 Sv range of observed values (Gordon et al. 1999).

The differences between the transport of the East Madagascar Current estimated by the POCM and by the observations (∼10 Sv) is smaller than the differences among the observational estimates themselves [e.g., a

20 Sv difference between the estimates of Lutjeharms et al. (1981) and those of Swallow et al. 1988]. The agreement between the model and observations seems reasonable, considering the fact that Table 1 compares a highly smoothed mean value from the model with short-period observations. The potential effect of transients on the mean calculation can be qualitatively appreciated by comparing the climatological mean in Fig. 2 with the instantaneous snapshot shown in Fig. 1. It is not possible to extract the climatological mean from relatively short and irregularly spaced observations that are biased by energetic, short-period processes or the particular method used in the calculation (e.g., the dynamic method). This is not to say that POCM-simulated values are better than the actual observations but that, considering the obvious shortcomings of both model and observations, the agreements appear to be robust. Model and observations can, of course, agree for the wrong reasons. To rule out such a possibility it is necessary to understand the physical processes that determine the mean circulation and its seasonal cycle in the model, and to asses the likelihood that the same processes occur in the real ocean.

b. The seasonal cycle

To illustrate the seasonal evolution of the currents depicted in Fig. 2 we calculated the POCM monthly transport anomalies by subtracting the annual mean value from the monthly climatology. The resulting time series are shown in Fig. 5, where the panels are arranged according to the geographical regions that they represent. Since all the currents in Fig. 5 have negative mean transports, a positive (negative) anomaly implies a decrease (increase) of its total value.

To facilitate our description of the tropical circulation we refer to the westward flow north of Madagascar as the North Madagascar Current (e.g., Kindle 1991). The
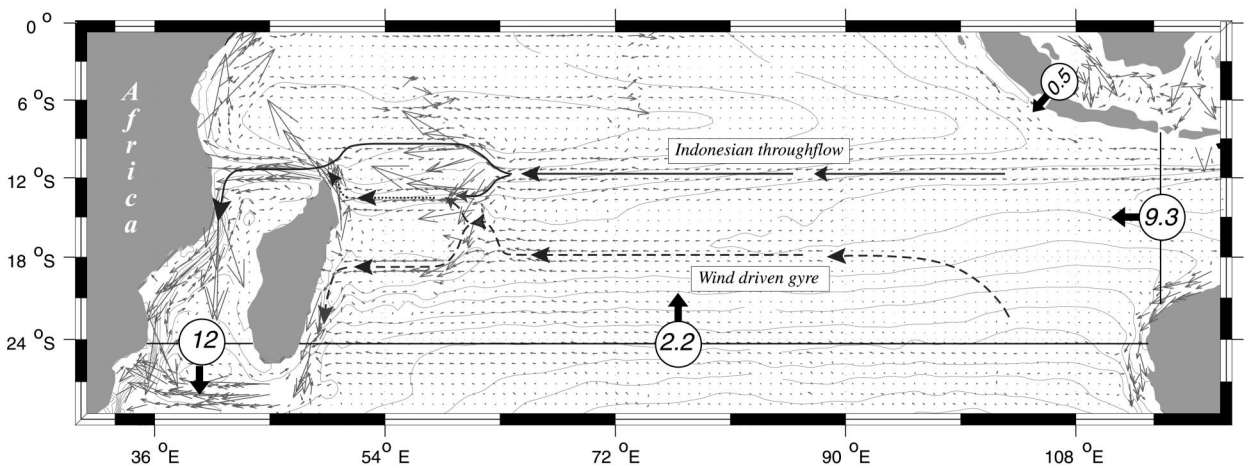

FIG. 4. Volume balance of the south Indian Ocean. The background vectors correspond to the climatological mean velocities in the POCM. The schematic arrows illustrate the pathway of the mean flow.
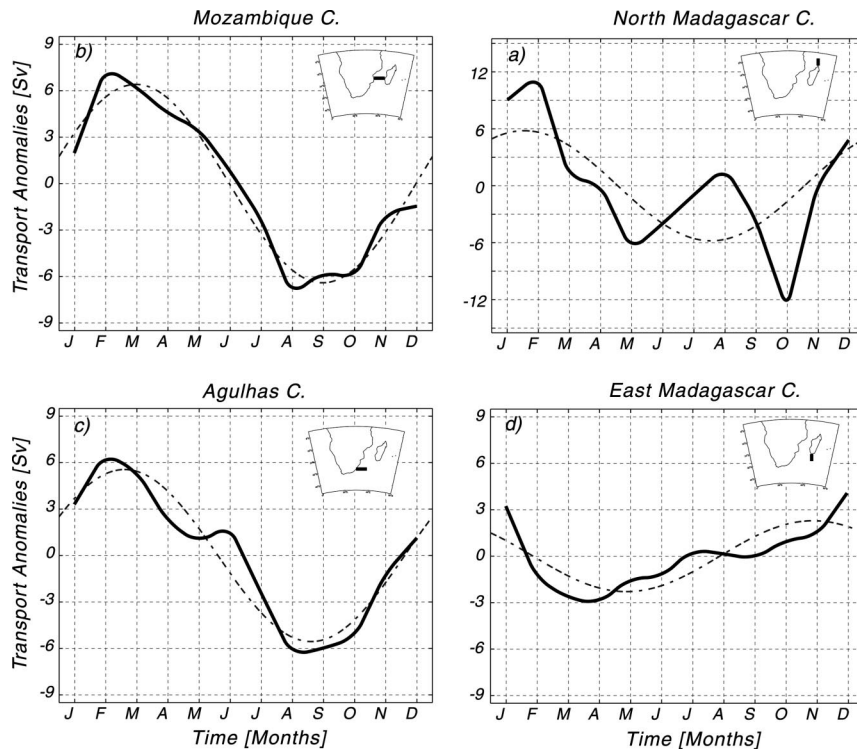
FIG. 5. Seasonal evolution of climatological transport anomalies (solid line) and its annual fit (dotted line) in the (a) North Madagascar Current, (b) Mozambique Current, (c) Agulhas Current, and (d) East Madagascar Current.

westward transport of the North Madagascar Current has a maximum at the beginning of the austral spring (September) and a minimum during the austral summer (Fig. 5a). The seasonal signal explains 20% of its total variance. The transports of the Mozambique and Agulhas Currents have a minimum during the austral summer (February) and a maximum at the end of the austral winter (August–October) (Figs. 5b,c). The peak-to-peak variations of the transports of these two currents is near 10 Sv, and the seasonal harmonic explains 39% of the variance of the Mozambique Current and 30% of the Agulhas Current. The East Madagascar Current also undergoes a small seasonal transition with a maximum at the end of the summer (March–April) and a minimum at the end of the spring (December–January) (Fig. 5d), although the seasonal harmonic only accounts for 12% of its total variance.

There are clear seasonal signals in the transports of the North Madagascar (Fig. 5a), Mozambique (Fig. 5b), and Agulhas (Fig. 5c) Currents. It is interesting to note that although the monthly evolution of the North Madagascar Current contains both annual and semiannual components, only the annual signal propagates southward. In fact, of the 20 Sv of transport variation observed north of Madagascar, only half reaches the Agulhas Current. The seasonal variation in the transport of the East Madagascar Current (Fig. 5d) is significantly

smaller than and out of phase with those in the other currents.

There are no long time series of observations to unequivocally define the seasonal cycle of the currents in the western Indian Ocean. Table 2 compares the seasonal variations from existing observations with the volume transports simulated by the model. For the sake of completeness, Table 2 includes the observations that Swallow et al. (1988) and Schott et al. (1988) collected north of Madagascar, although the latitudinal ranges used to calculate the model transports in that region are wider than those used in the observations. The estimates of Swallow et al. (1988) and Schott et al. (1988) were based on observations collected between 10° and 12°S (the Cape Amber Current), while our estimates extend from 7° to 12°S. The reason for using a wider latitudinal span is that while the narrow coastal current, surveyed by Swallow and Schott, appears to have little dynamical significance for the flow within the Mozambique Channel, the southern branch of the South Equatorial Current is the source of the seasonally propagating signal. It should be noted, with regards to this, that if the POCM transports are recalculated using only the near-shore points then the seasonal signal nearly disappears (Fig. 6, line with stars), in agreement with Swallow and Schott's observations. The seasonal signal observed in the modeled North Madagascar Current is consistent

TABLE 2. Seasonal variations of the current system in the western Indian Ocean according to observations and the POCM.

Current	Author	Variable	Maximum	Minimum
Agulhas	Pearce and Gründlingh (1982)	Surface velocity	None	None
	Ffield et al. (1997)	SSH transport at 32°S	Mar and Sep	Jun and Dec
		Hydrographic transport	Winter	Summer
	ECMWF	Wind curl at 30°S	Winter	Summer
	Quartly and Srokosz (1993)	SSH (Geosat)	Summer	Winter
	Matano et al. (1998)	SSH (TOPEX/Proseidon)	Summer	Winter
	Gründlingh (1980)	Geostrophic velocity	Fall/Winter	Summer
	POCM	Transport at 32°S	Winter/Spring	Summer
Mozambique	POCM	Transport	Winter	Summer
North Madagascar	Swallow et al. (1988)	Velocity (surface)	Spring	Summer
		Velocity ($z < 200$ m)	None	None
	Schott et al. (1988)	Transport	None	None
	POCM	Transport	Mar	Oct
East Madagascar	Swallow (1988)	Velocity	None	None
	Schott et al. (1988)	Transport	None	None
	POCM	Transport		

with the observations of Saetre (1985) and Hastenrath and Greischar (1991), who observed that the South Equatorial Current attains its maximum speeds in the winter.

There is qualitative agreement between model and observations on the lack of significant seasonal variations of the East Madagascar Current transport (Fig. 5d). Swallow et al. (1988) and Schott et al. (1988) reported the absence of significant seasonal changes in both geostrophic calculations and direct current meter deployments at 23°S. Swallow et al. (1988) pointed out that this is surprising considering the strong seasonal component of the atmospheric forcing. Matano et al. (1999) related the lack of seasonal variations in the southwestern Indian region to the effect of the bottom topography on the propagation of the seasonal signal. They argued that the oceanic response to seasonal

changes in the wind forcing at annual periods is mostly in a barotropic mode and that this mode is trapped in the interior of the basin.

The seasonal cycle of the Agulhas Current is characterized by a minimum of 37 Sv at the end of February and a maximum of 48 Sv that extends from August to October (Fig. 5c). Gründlingh (1980) calculated geostrophic transports of the Agulhas flow (relative to 1000 m) and found maxima during the fall/winter seasons and minima during the spring/summer. Pearce and Gründlingh (1982) later showed that Gründlingh's seasonal signal disappeared if the geostrophic calculations were referred to surface velocities. Ffield et al. (1997) calculated geostrophic transports using hydrographic and altimeter data. Their hydrographic calculations were referred to a level of 2000 db, and they found that the Agulhas transport is 7 Sv larger during the austral winter (June) than during the summer (March). Ffield et al. pointed out that this seasonality was reversed if the calculation was extended farther offshore (due to the presence of a strong cyclonic eddy). Unlike the hydrographic calculation, the transport estimates using SSH data indicated the dominance of a semiannual component with maxima at the end of summer and winter (March and August) and minima during summer and fall (December and May).

The hydrographic calculations of Gründlingh (1980) and Ffield et al. (1997) agree qualitatively with the model results. The main discrepancy between the POCM and the study of Ffield et al. (1997) is the semiannual signal observed in the latter. We do not have a clear explanation for this, but it is possible that their short-term observations may have been influenced by a recirculation cell that links the southern sector (dominated by winds with a stronger semiannual component) to the midlatitudes. Although such a cell is known to exist at times (e.g., Stramma and Lutjeharms 1997), it is not obvious whether it will also have the same effect on a
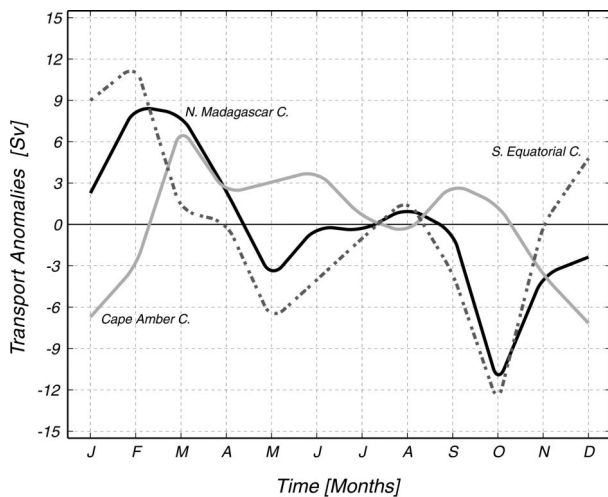

FIG. 6. Seasonal evolution of the climatological transport anomalies for the (a) North Madagascar Current, (b) Coast Cape Amber Current, and (c) South Equatorial Current.

longer-term climatology; if so, its effects are missing in the POCM.

Before closing our discussion on the comparison between the model and observations it is interesting to note that the seasonal changes in the Agulhas transport observed in the POCM are mostly in phase with those derived from the wind stress curl (Table 2). Although this may appear to be symptomatic of a midlatitude Sverdrup balance, in the following section we argue that the seasonal adjustment of the south Indian Ocean is instead driven by the variability of the tropical region.

4. Dynamics

According to the Sverdrup theory, the transport of a western boundary current is proportional to the zonal integral of the wind stress curl. Although the Sverdrup balance is a valid zero-order approximation to the mean transport, seasonal variations of the wind curl do not necessarily cause seasonal variations of the western boundary current transport. The basic argument, explained in detail in Gill and Niiler (1982) and Anderson and Corry (1984), is that the oceanic waves responsible for the adjustment of the ocean circulation to changes in the wind stress forcing are either too slow or too sensitive to bottom topography to effectively transmit information from the interior of the basin to the western boundary region. Kindle (1991) conducted a series of numerical experiments to investigate the seasonal cycle of the tropical region. According to his experiments most of the (predominately barotropic) seasonal signal that is generated in the eastern portion of the tropical south Indian Ocean is either unable to reach the western boundary currents or is reflected at the Mascarene Plateau. Matano et al. (1999) argued that the seasonal adjustment of the midlatitude basin could be decomposed into a series of basin modes whose spatial structure depends on the bottom topography. In particular, they hypothesized that the region of the Agulhas retroflection (i.e., the region south of 30°S and west of the Madagascar Ridge) is largely unaffected by the basin-scale wind variations but highly dependent on the local wind stress forcing. This hypothesis seems to be corroborated by the observed lack of correlation between the variations of the East Madagascar and Agulhas Currents in the POCM (Figs. 5c and 4d).

Since most of the volume flux from the tropical Indian Ocean through the Mozambique Channel is balanced by inflows from the Indonesian passages (Fig. 4), it seems reasonable to investigate whether the variability of the two regions are linked at seasonal timescales. We calculated the seasonal evolution of the transport anomalies of the Indonesian Throughflow (Fig. 7). The harmonic fit to the time series indicates that the annual component of the Indonesian Throughflows peaks in July with a westward anomaly of approximately 4 Sv. This result agrees with previous reports, which indicate that the Indonesian Throughflow varies seasonally, having a
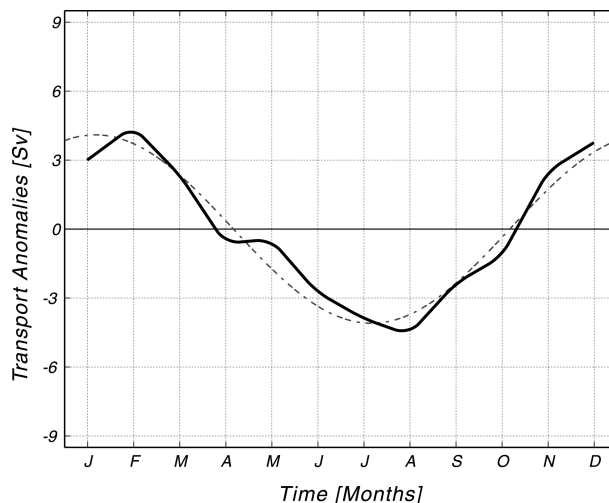

FIG. 7. Seasonal evolution of the transport anomalies of the Indonesian Throughflow. The dotted line marks the annual harmonic.

maximum during the austral winter and a minimum during the austral summer (Kindle et al. 1989; Inoue and Welsh 1993). Seasonal changes of the Indonesian Throughflow should be transmitted to the western boundary through the propagation of barotropic and baroclinc waves. An analysis of phase relations, however, fails to show linkages between these regions. It is easy to rationalize the lack of barotropic propagation by considering the inhibiting effect of bottom topography on the propagation of a barotropic signal (e.g., Kindle 1991). Furthermore, since most of the Indonesian Throughflow is highly baroclinic (strongly trapped in the upper layers) it is expected that most of its variability would project onto baroclinic waves.

It is more difficult to disregard the possibility of baroclinic connections between the eastern and western boundaries. A simple calculation indicates that in the tropical region Rossby waves can cross the basin in approximately one year. At 10°S, for example, a first baroclinic mode with a phase speed of approximately 0.2 m s^{-1} should cross a longitudinal range of 70° in approximately 440 days. Such a wave, if able to freely propagate, should create a phase difference between the seasonal variations of the two regions of approximately two months, a value close to the differences observed in the model output. Although it would be interesting to find dynamical connections between seasonal variations of the Agulhas transport and the Indonesian Throughflow, we found none. Instead, we found that the propagating patterns at the seasonal timescale are strongly constrained within sub-basins delimited by the bottom topography. To illustrate this point Fig. 8 shows time–longitude sections of the annual signal extracted from the model SSH anomalies. The topographic features with the most obvious influence on the wave propagation are the Mid-Indian Ridge (a quasi-meridional ridge located between 70° and 75°E), and the Mascarene
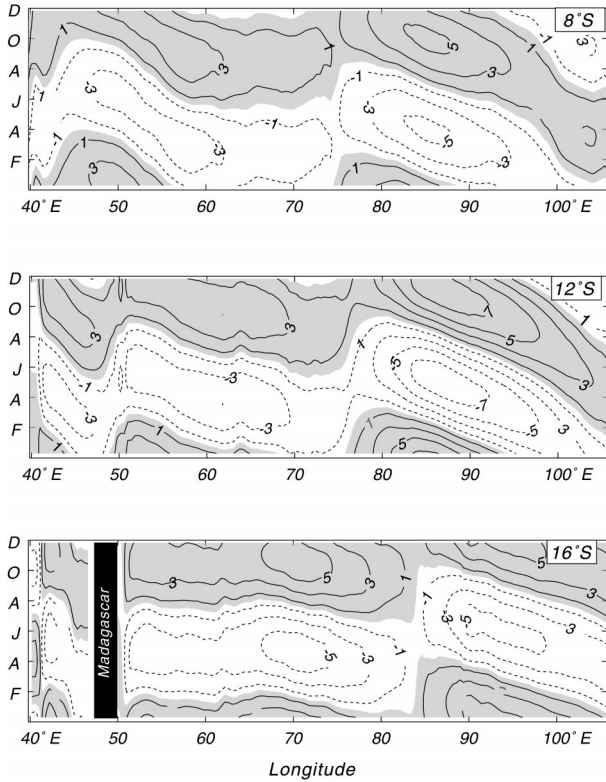
FIG. 8. Time–longitude plots of the annual component of the SSH anomalies at different latitudinal sections.

Plateau (an arch of small islands centered at approximately 60°E) (Fig. 9). The sections at 8° and 12°S show distinctive propagating patterns at the eastern (110°–85°E), and western (65°–40°E) regions, and no evidence of propagation in the central portion of the basin (85°–65°E). The westward-propagating signal in the eastern region fades to the west of the Ninety East Ridge. Over

the western region the propagating signal seems to originate over the Chagos Archipelago. Overall there is no indication of any coherent signal transmitting energy from the eastern to the western boundary.

To investigate whether the propagating SSH patterns correspond with changes of the transport of the South Equatorial Current we calculated time series of the transport anomalies (Fig. 10). In agreement with our previous results, Fig. 10 shows that the transport of the South Equatorial Current has a seasonal signal that propagates from the Indonesian passages to 80°E, with a phase lag of approximately 4 months. Between 80° and 70°E the westward-propagating signal is lost.

The previous analysis indicates that, at seasonal time-scales, the variabilities of the eastern and western regions of the Indian Ocean are largely uncoupled. In what follows we will try to explain the seasonal variability of the Indian Ocean using the concept of barotropic modes, the rationale being that relatively fast changes of the wind forcing (periods of one year or less) set up barotropic currents that rapidly propagate the wind forcing within subregions of the basin that are delimited by ridges or plateaus (e.g., Anderson and Killworth 1977). To identify the spatial and temporal structure of these modes we will use harmonic analysis and empirical ortoghonal functions (EOFs).

a. Harmonic analysis

To characterize the spatial and temporal structure of the seasonal variability in the Indian Ocean we fitted an annual harmonic to the SSH data (Fig. 11). North of 20°S, the harmonic's amplitude defines three regions with maxima delimited by amphidromic lines. The western region, which extends from Africa to the middle of the basin, is characterized by a maximum along the coast that represents the seasonal cycle of the South Equa-
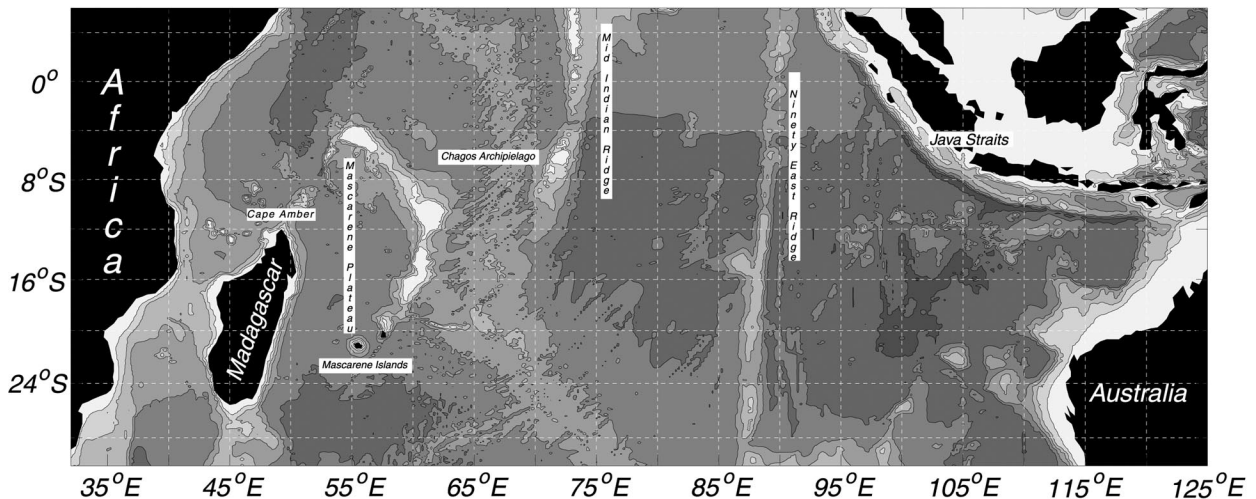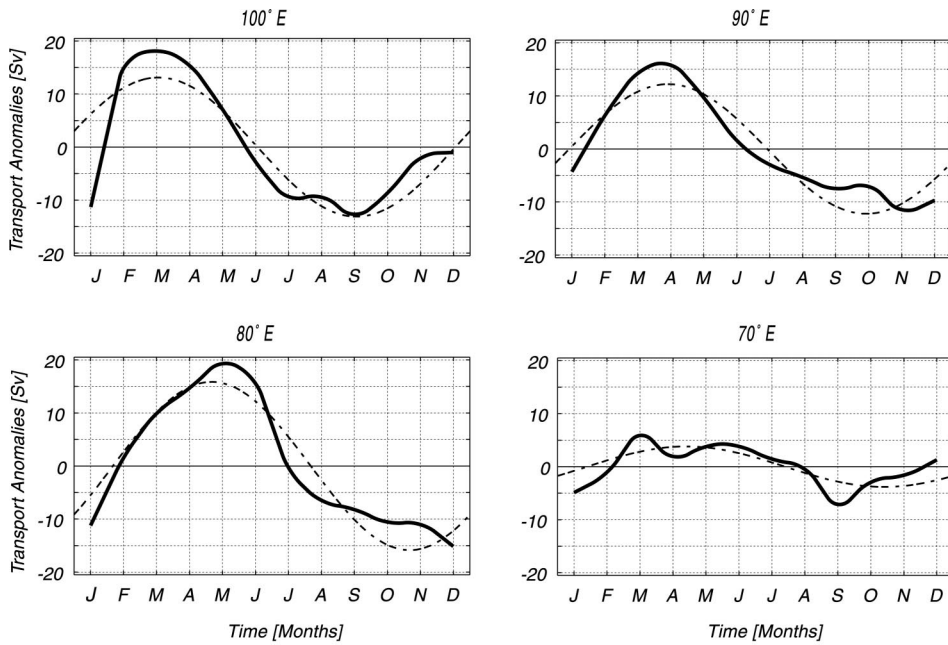

FIG. 9. Bottom topography of the south Indian Ocean.

FIG. 10. Seasonal evolution of the transport anomalies of the branch of the South Equatorial Current that connects to the Indonesian passages. See Fig. 2 for the locations of the sections.

torial Countercurrent. The central region contains the seasonal signal with the largest amplitude within the Indian Basin, accounting for almost 60% of the local variance. This SSH maximum corresponds with a maximum of the wind stress curl. The eastern region is mostly restricted to the Indonesian passages, and its

maximum is related to the seasonal cycle of the Indonesian Throughflow.

The separated SSH maxima in the western and central regions of Fig. 11 indicate that the annual variabilities of those regions are not correlated. The phase lines of the central region, for example, indicate westward prop-
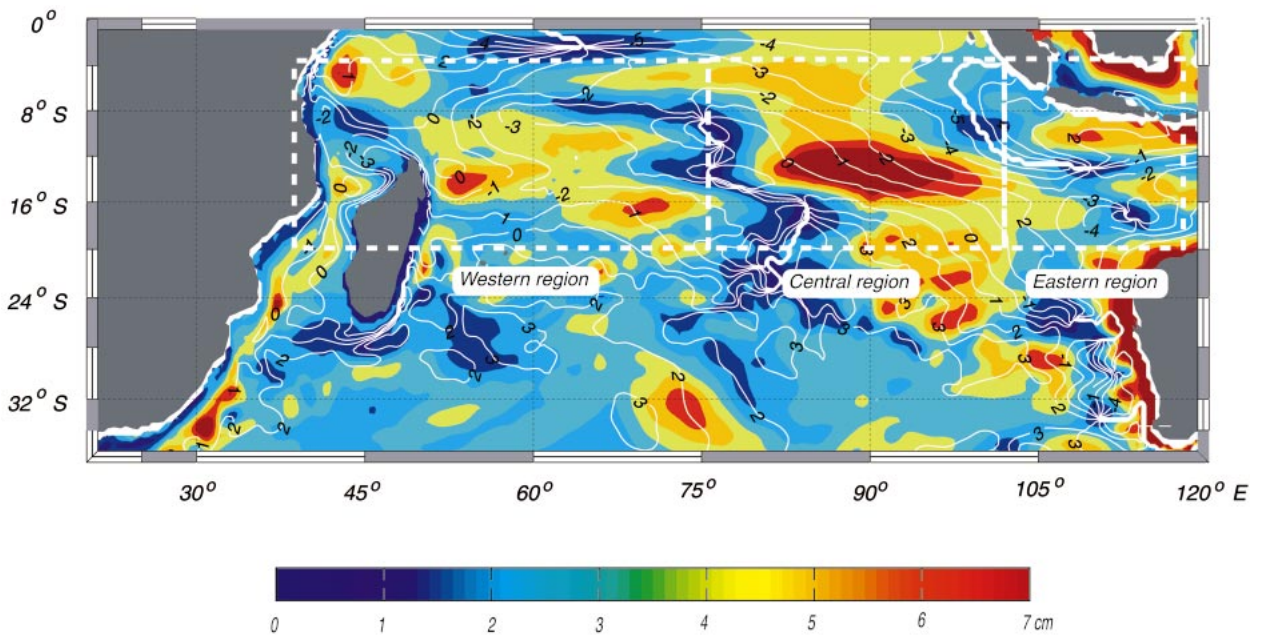

FIG. 11. Amplitude (color background) and phase (white lines) of the annual harmonic fit to the POCM SSHs in the south Indian Ocean. The values of the phases are given in months, with 15 Dec as reference.
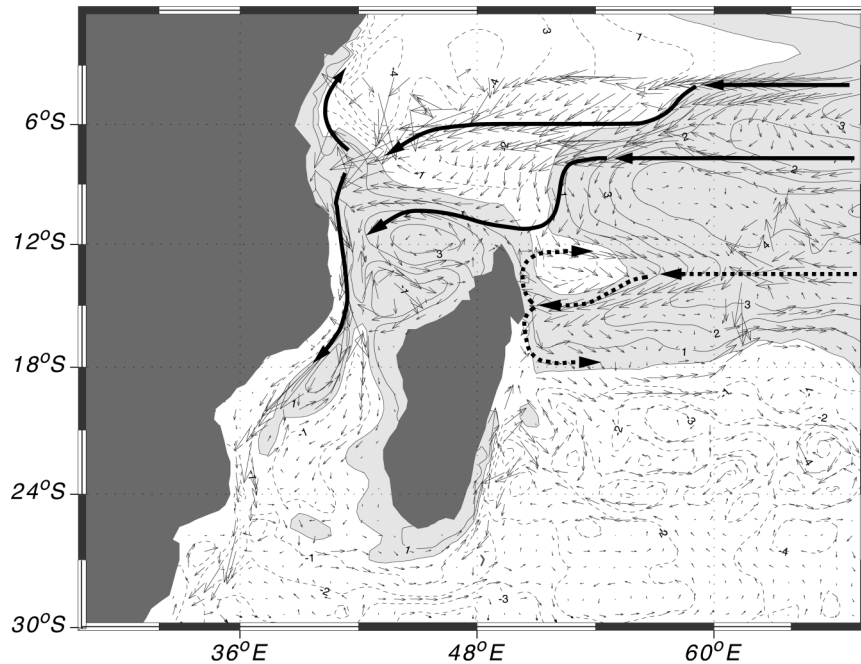
FIG. 12. Amplitude of the annual harmonic fit to (a) SSH (solid lines) and (b) 1000-m averaged velocities (vector arrows). The schematic arrows mark the pathways of the seasonal signal.

agation with an approximate lag of 4 months between 105° and 75°E. The westward propagation halts at the amphidromic line located near 75°E. This line follows the contours of the Mid-Indian Ridge in the tropical and equatorial regions and the Ninety East Ridge at midlatitudes (Fig. 9). The seasonal signal of the western region appears to originate over these topographic formations and propagate westward with an approximate time lag of 4 months between Madagascar and the center of the basin.

To illustrate the connection between the western boundary region and the interior circulation Fig. 12 shows the August component of the annual harmonic for velocities and SSHs. This figure shows that the seasonal signal that gets to the Mozambique Channel, and eventually to the Agulhas Current, has its origins in the tropical region and not in the midlatitudes. In fact, as schematically illustrated by the black arrows superimposed on Fig. 12, the branch of the South Equatorial Current that feeds the East Madagascar Current (dotted arrows) reflects along the coast of Madagascar and does not influence the northernmost portion of the island. The circulation patterns depicted in Fig. 12 offer a possible explanation as to why there is no clear seasonal signal in the coastal region off Madagascar (e.g., Fig. 6), while there is a well-defined annual component farther offshore that correlates well with the annual signal in the Mozambique Channel (Figs. 5a,b).

b. EOF analysis

To further investigate the spatial and temporal structure of the Indian Ocean variability we calculated the EOFs of the POCM SSH anomalies. Figure 13 shows the spatial and temporal structure of the first three modes, which account for approximately 40% of the variance. The arrows superimposed on Fig. 13a represent the geostrophic velocities associated with the SSH gradients. In general the spatial structure of the EOF modes corresponds well with the structure of the annual harmonic. The first EOF mode (Fig. 13a), which accounts for approximately 17% of the total variance, contains two SSH maxima. The westernmost of these maxima is located between the equator and 6°S and it represents the seasonal cycle of the South Equatorial Countercurrent system. The second maximum of the first mode is located in the center of the basin, and it is associated with a maximum in the wind stress curl. In this region the seasonal variability accounts for more than 60% of the total variance.

The second EOF mode, which explains approximately 15% of the variance, is the one that appears to be more related to the variability in the northwestern region. The spatial structure of this mode (Fig. 13a) shows the maxima in the western and central regions that closely correspond with those of the annual harmonic (Fig. 11). The separation between the EOF maxima roughly follows the bottom topography. Unlike the annual harmonic, however, where the two maxima are clearly separated by a region of zero amplitude and an amphidromic line, the EOF structure indicates some linkages between the regions of maximum variability. In this regard it should be remembered that, unlike the annual harmonic, which isolates the spatial and temporal structure of anomalies with only that frequency component, the
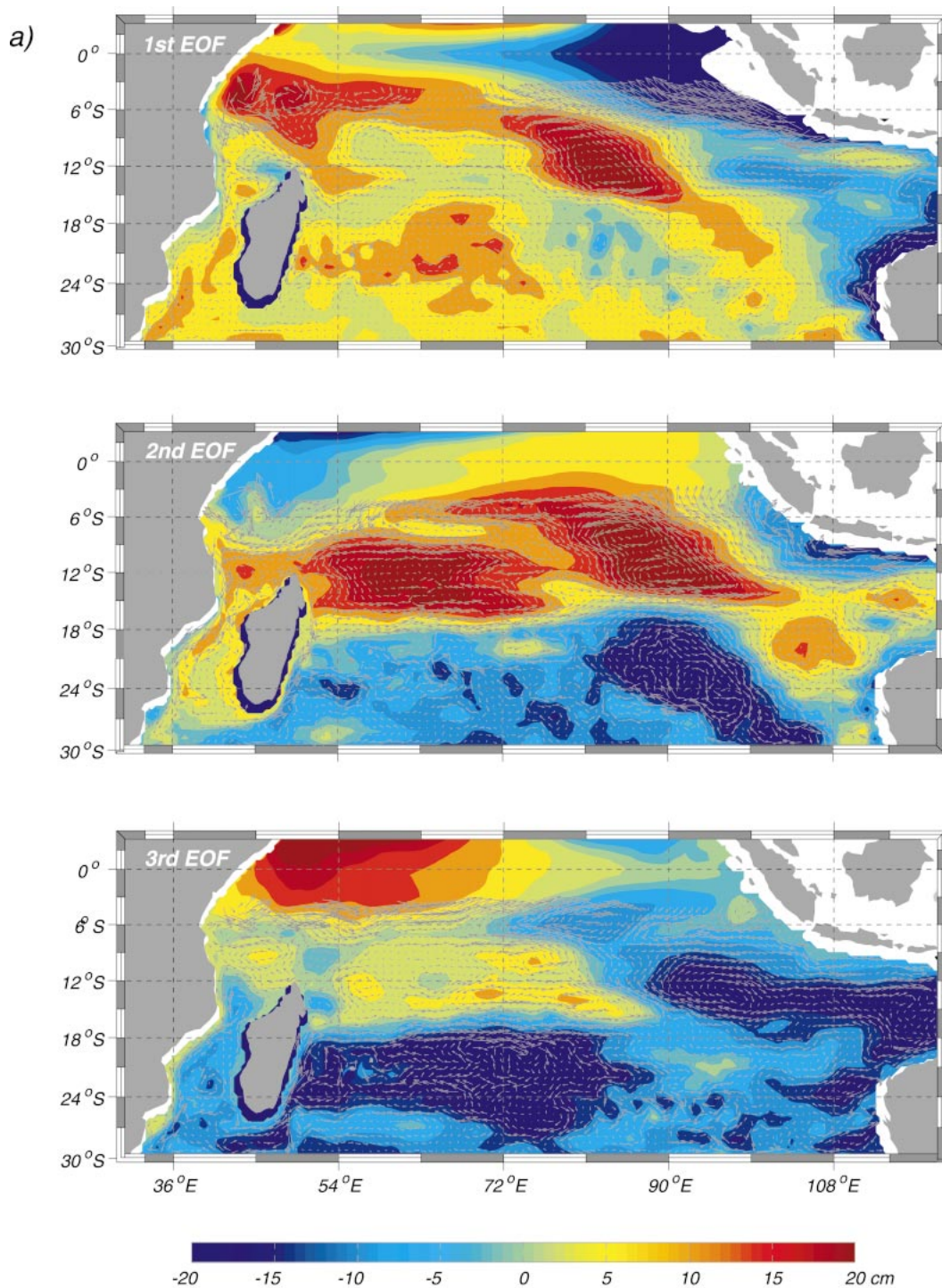
FIG. 13. The first three EOFs' modes of the SSH variability in the south Indian Ocean: (a) spatial structure of the amplitude (with superimposed geostrophic velocities); (b) time series.

EOFs summarize the information about all the existing frequencies. The EOFs therefore, show linkages due to processes associated with timescales other than the annual (e.g., the propagation of eddies at interannual time periods or interannual changes in the Indonesian Throughflow).

The spatial structure of the third mode in the eastern section of the basin can be associated with the Indo-
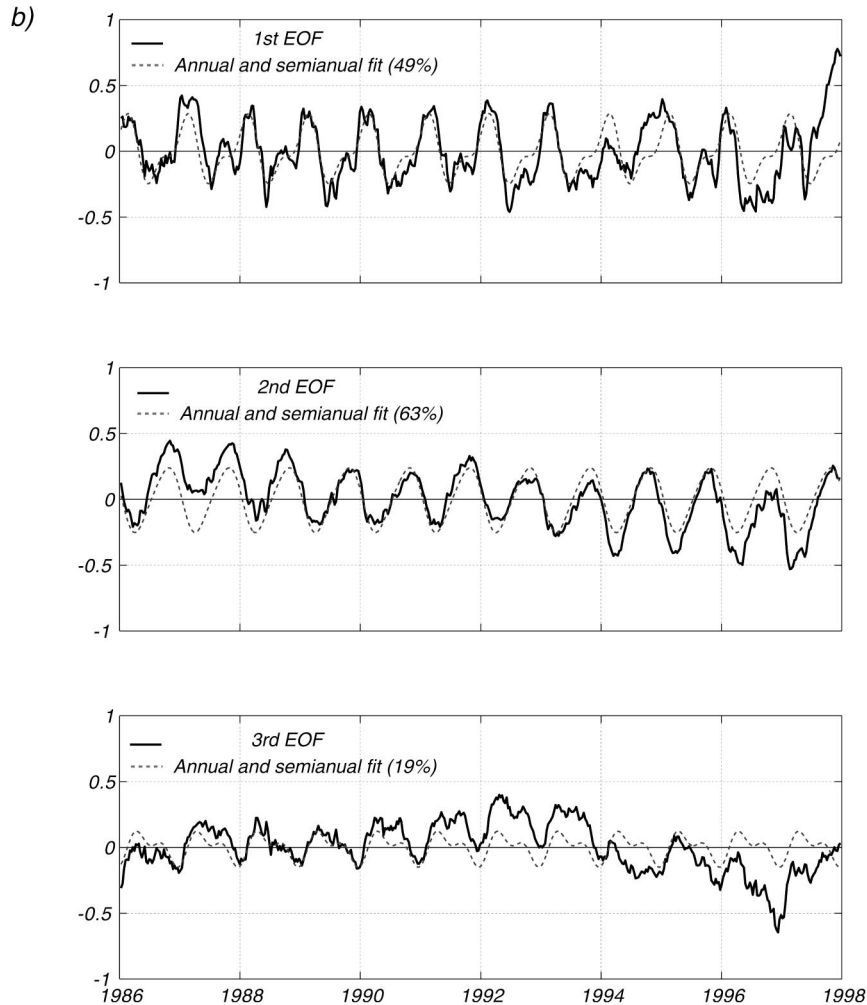
FIG. 13. (*Continued*)

nesian Throughflow. It consists of an SSH anomaly tongue that extends in a northwest direction from the Indonesian passages to the center of the basin. Our previous analysis of the fate of the SSH perturbations caused by the seasonal variations of the Indonesian Throughflow shows that, at the annual scale, these perturbations flow westward to the longitude of the Ninety East Ridge (Fig. 9), where they are diverted into a northwestward direction to lower latitudes. Most of these perturbations appear to project into the third EOF mode, which has a maximum in the northeastward portion of the basin.

The temporal structure of each of the EOFs with their annual and semiannual fits is depicted in Fig. 13b. Although the EOFs summarize information from all the existing frequencies, the time series of each mode is strongly dominated by the annual cycle. Note that the second EOF leads the first by several months. This is consistent with the interpretation that the central maximum in the second (first) EOF represents the eastern (western) part of the central region maximum in the

annual harmonic. The propagation across this maximum takes between 3 and 4 months. It is interesting to note that since the second EOF has a better fit than the first to the annual and semiannual harmonics (63% against 49% of the first EOF) it actually explains a slightly larger percentage of the total seasonal variability. In terms of the local variance, the first and second EOF modes explain 50% of the total variance of the Mozambique Channel.

5. Summary and conclusions

In this article we examined the kinematics and dynamics of the seasonal cycle of the south Indian Ocean in an eddy-permitting global simulation. The focus of our study was the western region, where we linked the seasonal changes of the transport of the Agulhas Current to the large-scale circulation in the tropical region. In agreement with the modeling study of Biastoch et al. (1999), the transport of the Agulhas Current in the POCM has a seasonal variation with a maximum at the
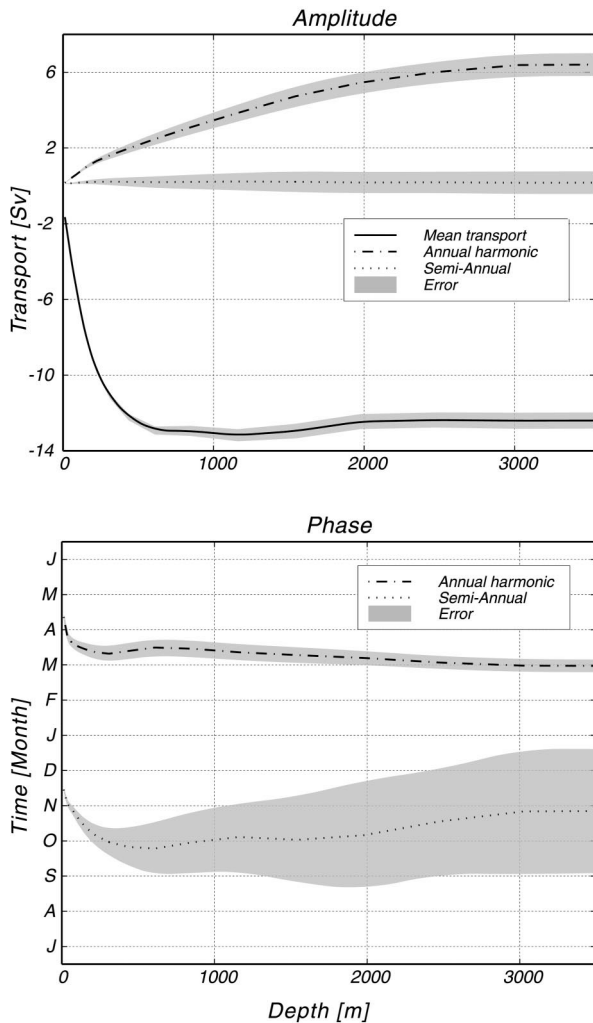
FIG. 14. Vertical structure of the mean transport of the Mozambique Current and the amplitude and phase of the annual and semiannual harmonic fits to its variability.

tion of the basin. The second, located in the center of the basin, appears to be closely related to the local winds. The third mode is restricted to the western portion of the basin and affects the variability of two distinct regions. To the southwest it includes the Mozambique Channel and its connection to the South Equatorial Current. To the north it appears to be associated with the strong seasonal cycle of the South Equatorial Current. The driving force for all of these modes, except that associated with the Indonesian Throughflow, appears to be the wind forcing. Although it is tempting to identify these modes of variability with the normal modes of a basin, the comparison can be deceiving since baroclinic and nonlinear processes link these modes.

Anderson and Killworth (1977) have discussed in detail the mechanisms by which regional modes can be generated. They showed that sudden changes in the wind forcing will set up barotropic currents that rapidly propagate the wind information within subregions of the basin that are delimited by ridges or plateaus. There is general agreement between these theoretical predictions and model results. Figure 14 shows, as an example, the amplitude and phase of the vertical structure of the mean transport through the Mozambique Channel and its annual and semiannual components. In agreement with theory, Fig. 14 shows that although the mean transport in the Mozambique Channel is highly baroclinic, mostly confined to the upper 500 m, its variability is highly barotropic, reaching up to depths of 3000 m.

With obvious caveats, the simulated current transports appear to compare favorably with observations, except in the Mozambique Channel. There the POCM indicates the existence of a poleward mean transport caused by the poleward propagation of eddies. The structure of the mean flows generated by these eddies can not be validated by the scant data of the region [although the transports within the Mozambique Current recently reported by de Ruijter et al. (2002) are in close agreement with those derived from the POCM].

transition between the austral winter and the austral spring and a minimum between the austral summer and the austral autumn. Regional and basin-scale mass balances indicate that, although the mean flow of the Agulhas Current has a substantial contribution from the Indonesian Throughflow, there are no obvious dynamical linkages between the seasonal oscillations of these two currents. We can not prove conclusively that they do not exist, only that we have not been able to find them. Instead, we found evidence that the seasonal cycle of the western Indian Ocean is the result of the oscillation of barotropic modes forced by the wind in the same region.

The results of the harmonic and EOF analyses indicate that the structure of the seasonal variability in the tropical South Indian Ocean can be rationalized in terms of three regional modes. The first, associated with the Indonesian Throughflow, is restricted to the eastern por-

REFERENCES

Anderson, D. L. T., and P. D. Killworth, 1977: Spin-up of a stratified ocean with topography. *Deep-Sea Res.,* **24,** 709–732.
——, and R. A. Corry, 1984: Ocean response to low frequency forcing with application to the seasonal variations in the Florida-Straits–Gulf Stream transports. *Progress in Oceanography,* Vol. 14, Pergamon, 7–40.
Beal, L. M., and H. L. Bryden, 1999: The velocity and vorticity structure of the Agulhas Current at 32°S. *J. Geophys. Res.,* **104,** 5151–5176.
Biastoch, A., and W. Krauss, 1999: The role of mesoscale eddies in

the source regions of the Agulhas Current. *J. Phys. Oceanogr.,* **29,** 2303–2317.

——, C. J. C. Reason, J. R. E. Lutjeharms, and O. Boebel, 1999: The importance of flow in the Mozambique Channel to seasonality in the greater Agulhas Current System. *Geophys. Res. Lett.,* **26,** 3321–3324.

de Ruijter, W. P. M., A. Biastoch, S. S. Drijfhout, J. R. E. Lutjeharms, R. P. Matano, T. Pichevin, P. J. van Leeuwen, and W. Wijer, 1999: Indian–Atlantic interocean exchange: Dynamics, estimation and impact. *J. Geophys. Res.,* **104,** 20 885–20 910.

——, H. Ridderinkhof, J. R. E. Lutjeharms, and M. W. Schouten, 2002: Observations of the flow in the Mozambique Channel. *Geophys. Res. Lett.,* in press.

Ffield, A., J. Toole, and D. Wilson, 1997: Seasonal circulation in the South Indian Ocean. *Geophys. Res. Lett.,* **24,** 2773–2776.

Fu, L.-L., 1986: Mass, heat and freshwater fluxes in the South Indian Ocean. *J. Phys. Oceanogr.,* **16,** 1683–1693.

Gill, A. E., and P. P. Niiler, 1982: The theory of the seasonal variability in the ocean. *Deep-Sea Res.,* **20,** 141–177.

Godfrey, J. S., 1989: A Sverdrup model of the depth-integrated flow for the world ocean allowing for island circulations. *Geophys. Astrophys. Fluid Dyn.,* **45,** 89–112.

Gordon, A. L., R. D. Susanto, and A. Ffield, 1999: Throughflow within Makasaar Strait. *Geophys. Res. Lett.,* **26,** 3325–3328.

Gründlingh, M. L., 1980: On the volume transport of the Agulhas Current. *Deep-Sea Res.,* **27,** 557–563.

Harris, T. F. W., 1972: Sources of the Agulhas Current in the spring of 1964. *Deep-Sea Res.,* **19,** 633–650.

Hastenrath, S., and L. Greishar, 1991: The monsoonal current regimes of the tropical Indian Ocean: Observed surface flow fields and wind driven components. *J. Geophys. Res.,* **96,** 12 619–12 633.

Inoue, M., and S. E. Welsh, 1993: Modeling seasonal variability in the wind-driven upper-layer circulation of the Indo-Pacific region. *J. Phys. Oceanogr.,* **23,** 1411–1436.

Kindle, J., 1991: Topographic effects on the seasonal circulation of the Indian Ocean. *J. Geophys. Res.,* **96,** 16 827–16 837.

——, H. E. Hurlburt, and E. J. Metzger, 1989: On the seasonal and interannual variability of the Pacific to Indian Ocean throughflow. *Proc. Western Pacific Int. Meeting and Workshop on TOGA COARE,* Noumea, New Caledonia, Centre ORSTOM de Nouméa, 355–365.

Lutjeharms, J. R. E., N. D. Bang, and C. P. Duncan, 1981: Characteristics of the currents east and south of Madagascar. *Deep-Sea Res.,* **28,** 879–899.

——, P. M. Wedepohl, and J. M. Meeuwis, 2000: On the surface drift of the East Madagascar and Mozambique Currents. *South Afr. J. Sci.,* **96,** 141–147.

Matano, R. P., C. G. Simionato, W. P. de Ruijter, P. J. van Leeuween, P. T. Strub, D. B. Chelton, and M. G. Schlax, 1998: Seasonal variability in the Agulhas retroflection region. *Geophys. Res. Lett.,* **25,** 4361–4364.

——, ——, and P. T. Strub, 1999: Modeling the wind-driven variability of the South Indian Ocean. *J. Phys. Oceanogr.,* **29,** 217–230.

Pearce, A. F., and M. L. Gründlingh, 1982: Is there a seasonal variation in the Agulhas Current? *J. Mar. Res.,* **40,** 177–184.

Quartly, G. D., and M. A. Srokosz, 1993: Seasonal variations in the region of the Agulhas retroflection: Studies with Geosat and FRAM. *J. Phys. Oceanogr.,* **23,** 2107–2124.

Saetre, R., 1985: Surface currents in the Mozambique Channel. *Deep-Sea Res.,* **32,** 1457–1467.

Schott, F., M. Fieux, J. Kindle, J. Swallow, and R. Zantopp, 1988: The boundary currents east and north of Madagascar. 2. Direct measurements and model comparisons. *J. Geophys. Res.,* **93,** 4963–4974.

Schouten, M. W., W. P. M. de Ruijter, and P. J. van Leeuwen, 2002: Upstream control of the Agulhas ring shedding. *J. Geophys. Res.,* in press.

Stammer, D., R. Tokmakian, A. Semtner, and C. Wunsch, 1996: How well does a 1/4° global circulation model simulate large-scale oceanic observations? *J. Geophys. Res.,* **101** (C10), 25 779–25 811.

Stramma, L., and J. R. E. Lutjeharms, 1997: The flow field of the subtropical gyre of the South Indian Ocean. *J. Geophys. Res.,* **102,** 5513–5530.

Swallow, J. C., M. Fieux, and F. Schott, 1988: The boundary currents east and north of Madagascar. 1. Geostrophic currents and transports. *J. Geophys. Res.,* **93,** 4951–4962.

Toole, J. M., and B. A. Warren, 1993: A hydrographic section across the subtropical South Indian Ocean. *Deep-Sea Res.,* **40,** 1973–2019.

van Leeuwen, P. J., W. P. M. de Ruijter, and J. R. E. Lutjeharms, 2000: Natal pulses and the formation of Agulhas rings. *J. Geophys. Res.,* **105,** 6425–6436.